



Phyto Fabrication of Silver Nanocomposites from *Ageratum conyzoides* as Potent Mosquitocidal and Antidengue Activity of *Aedes aegypti*

Christina Mary Samidoss^{a+++*}, Maryjoy Samidoss^{b#}
and Juliet Gnana Sundari^{ct}

^a Department of Zoology, Michel Job College of Arts and Science for Women, Sulur, Coimbatore, Tamilnadu, India.

^b PSG Arts and Science, Coimbatore, Tamilnadu, India.

^c JCT College of Engineering and Technology, Pichanur, Tamilnadu, India.

Authors' contributions

This work was carried out in collaboration among all authors. All authors read and approved the final manuscript.

Article Information

DOI: 10.56557/UPJOZ/2023/v44i123535

Editor(s):

(1) Dr. Pinar Oguzhan Yildiz, Ataturk University, Turkey.

Reviewers:

(1) Elsayed Eldeeb Mehana Hamouda, Alexandria University, Egypt.

(2) Dharmasoth Rama Devi, Dr. Samuel George Institute of Pharmaceutical Sciences, India.

Original Research Article

Received: 05/12/2022

Accepted: 09/02/2023

Published: 23/06/2023

⁺⁺ Assistant Professor;

[#] Research Scholar;

[†] Associate Professor;

*Corresponding author: Email: christina.mary@mjc.ac.in;

ABSTRACT

Mosquitoes pose an enormous threat to millions of people worldwide and transmit important diseases, including malaria, dengue, yellow fever, filariasis, Japanese encephalitis and the Zika virus. Currently, a growing number of phyto-synthesized silver nanoparticles (AgNPs) have recently been proposed as effective mosquito larvicides and are gaining traction over synthetic chemical pesticides due to their less deleterious effects on non-target species and novelty in mechanisms of action. The current study was conducted to evaluate the larvicidal and pupicidal activity of AgNP synthesized from *Ageratum conyzoides* against dengue vector *Aedes aegypti* as well as in vitro antiviral assay. The biosynthesized AgNPs were characterized using a UV-Vis spectrometer, powder X-ray diffraction (XRD), Fourier transform infrared spectroscopy (FTIR), scanning electron microscopy (SEM), and energy-dispersive X-ray spectroscopy (EDX). The mosquito larvae were tested with biosynthesized AgNPs and the LC50 values recorded were I-stage (20.451), II-stage (23.307), III-stage (27.397), IV-stage (33.351), and pupa (39.668), respectively. To screen the anti-dengue properties of *A. conyzoides*-synthesized AgNP, an in vitro antiviral assay was performed. The present research reported moderate cytotoxicity rates in Vero cells exposed to *A. conyzoides*-synthesized AgNP at various concentrations. From this we observed that no adverse morphological differences were found in the treated cells that were comparable to the control Vero cells. Overall, our results demonstrated that AgNPs synthesized by *A. conyzoides* can be used to design newer and safer dengue control agents.

Keywords: *Aedes aegypti*; silver nanoparticles; green synthesis; larvicidal; pupicidal; invitro analysis; eco-friendly.

1. INTRODUCTION

“Mosquitoes (Diptera: Culicidae) are a major threat to millions of people and animals around the world. Their medical and veterinary importance derives primarily from their role as vectors for a variety of public health pathogens and parasites, including malaria, avian malaria, yellow fever, dengue fever, Japanese encephalitis, Zika virus, Rift Valley fever, western equine encephalomyelitis, and Bancroftian Brugian Filariasis, Canine Heartworm Disease (*Dirofilaria immitis*) and Setariasis (*Setaria* spp.). Dengue is primarily transmitted by *Aedes* mosquitoes (i.e. *Aedes aegypti* and to a lesser extent *Aedes albopictus*). The true number of dengue cases is underreported and many cases are misclassified. 3900 million people in 128 countries are at risk of being infected with dengue viruses” [1]. “There is currently no specific treatment for dengue” [2,3].

“Therefore, new and safer, environmentally friendly strategies to combat mosquito vectors are urgently needed. Interestingly, the use of different plant compounds as reducing and stabilizing agents resulted in metal nanoparticles with different size, shape, and toxic properties against mosquito vectors. Nanobiotechnologies have the potential to revolutionize a wide range of applications including drug delivery, diagnostics, imaging, sensing, gene delivery, artificial implants, tissue engineering,

parasitology and pest control” [4]. “Plant-mediated biosynthesis of nanoparticles is advantageous over chemical and physical methods because it is cheap, in one step and without high pressure, energy, temperature and the use of highly toxic chemicals” [5].

Ageratum conyzoides (Asteraceae) aerial parts underwent a general phytochemical screening that identified the presence of alkaloids, terpenes, phenolic compounds, saponins, steroids, and steroid-like substances. It is used for a variety of folk medicinal purposes [6]. *A. conyzoides* is an annual herb that has a long history of being used traditionally as medicine in many nations, especially in tropical and subtropical areas. From ancient times, the plant has been used to cure a variety of illnesses, including burns and wounds, for its antibacterial properties, and for many infectious infections [6]. The objective of the current study, which used *A. conyzoides* as a model organism, was to assess the efficacy of biologically produced silver nanoparticles in the treatment of dengue vector *A. aegypti*.

2. MATERIALS AND METHODS

2.1 Collection of Plant

A. conyzoides plant was collected from Western Ghats region of The Nilgries, Southern India. The plants were identified at Botanical Survey of

India (TNAU) and the voucher numbered BSI/SRC/ 5/ 23/ 2017/ Tech. 1908 specimens were deposited at Zoology Department, Bharathiar University, and Coimbatore, India.

2.2 Preparation of Plant Extracts

10g of coarse powder of *A. conyzoides* were mixed in different solvents like distilled water, ethanol, hydro ethanol, acetone, chloroform and petroleum benzene separately and macerated for three days. During the maceration period, continuous stirring was done. After three days, the suspension was filtered using filter paper and a funnel. The filtrate was taken in a round bottomed flask and used for GC-MS analysis.

2.3 Gas Chromatography-Mass Spectroscopy Analysis

The ethanolic extract was analysed using the GC-MS SHIMADZU QP2010 instrument with the Elite - DB- 5M column and the GC-MS solution version 2.53 software. The oven temperature was initially kept at 70°C for 2.0 minutes before gradually increasing to 300°C at 10.0/35.0 minutes and injecting 4.0 µl of sample for analysis. Helium gas with a purity of 99.995% was used as both a carrier gas and an eluent. The helium gas flow rate was set to 1.5 ml/min. Throughout the experiment, the sample injector temperature was kept at 260°C, and the split ratio was set to 20. 70 eV was used for the ionization mass spectroscopic analysis. For about 35 minutes, mass spectra in the range 40-1000 m/z were recorded. The components were identified by comparing their mass spectra. "Electronic signals were detected as the compounds separated during elution through the column. Individual compounds eluted from the gas chromatographic column entered the electron ionization detector, where they were bombarded with electrons, causing them to fragment. The fragments were actually charged ions of varying masses. The m/z ratio obtained was calibrated using the graph obtained, known as the mass spectrum graph, which is the molecule's fingerprint. The identification of compounds was based on mass spectral comparisons with NIST Library 2008 WILEY8, FAME" [7].

2.4 Synthesis of Silver Nanoparticles

A. conyzoides leaf samples were cleaned in distilled water and allowed to air dry for two days. In a 300 ml flask, 10 g of finely chopped plant

leaves were combined with 100 ml of sterile distilled water to create a plant leaf broth. Before being utilised in testing, this combination was boiled for five minutes, decanted, and kept at -4°C for a week. "An Erlenmeyer flask containing the filtrate and a 1 mM aqueous AgNO₃ solution was then incubated at room temperature. As a result, a brown-yellow solution was found, showing the synthesis of AgNPs and the ability of an aqueous extract of plant materials to decrease aqueous silver ions to make extremely stable silver nanoparticles in water" [8].

2.5 Characterization of the *A. conyzoides* synthesized Silver Nanoparticles

By sampling the reaction mixture at regular intervals and analysing the absorption maxima using UV-Vis spectra at 200-800 nm in a Shimadzu UV-3600 spectrophotometer with a resolution of 1 nm, the production of silver nanoparticles was verified. After 20 minutes of centrifuging the reaction mixture at 15,000 rpm, the pellet that was produced was dissolved in deionized water and put through a Millipore filter (0.45 µm). An aliquot of this filtrate containing silver nanoparticles was subjected to SEM, energy dispersive spectroscopy (EDS), Fourier transform infrared spectroscopy (FTIR), X-ray diffraction (XRD), and energy dispersive X-ray spectroscopy (EDX). A 10 kV ultra-high resolution scanning electron microscope was used to investigate the structure and makeup of pure silver particles that had been freeze-dried. Using an FEI QUANTA-200 SEM, pictures of nanoparticles were analysed after a 25 L sample was sputter coated onto a copper die. Using a Perkin-Elmer Spectrum 2000 FTIR spectrophotometer, FTIR spectroscopy was used to qualitatively identify the surface groups of the nanoparticles. EDS analysis was also used to confirm the presence of metals in the samples under study [8].

2.6 Larvicidal and Pupicidal Experiments against *Aedes aegypti*

"For 24 hours, 25 *Ae. aegypti* larvae or pupae were placed in a 500 mL beaker filled with 250 mL of dechlorinated water, and 1 mL of the desired concentration of *A. conyzoides* extract or green synthesised silver nanoparticles was added. 0.5 mg larval food was provided for each concentration tested" [9]. Each concentration was tested against all stages five times. For 24 hours, control mosquitos were exposed to the

appropriate concentration of the solvent. The mortality rate was calculated as follows:

Percentage mortality = (number of dead individuals/numbers of treated individuals) *100

2.7 Antiviral Activity

2.7.1 Cell culture

The kidney cells of an African green monkey (Vero) were obtained from the National Center for Cell Sciences (NCCS) in Pune, India. Cancer cells were cultured in Dulbecco's Modified Eagles Medium (DMEM) supplemented with 2mM l-Glutamine and Balanced Salt Solution (BSS) supplemented with 1.5 g/l Na₂CO₃, 0.1mM non-essential amino acids, 1mM sodium pyruvate, 2 mM l-glutamine, 1.5 g/L glucose, 10 mM (4-(2-hydroxyethyl)-1-(GIBCO, USA), penicillin and streptomycin (100 IU/100 g) were adjusted to 1 mL/L. Cells were kept at 37°C with 5% CO₂ in a humidified CO₂ incubator.

2.7.2 Cytotoxicity assay

The following tests were carried out to determine the cytotoxicity of Ag nanoparticles. The cytotoxicity of the compounds was determined using an MTT assay [3-(4,5-dimethylthiazol-2-yl)-2,5-diphenyltetrazolium bromide]. Cells were grown to 75% confluency in a 96-well plate (1104 cells/well) for 48 hours. The cells were incubated for an additional 48 hours in fresh medium containing serially diluted synthesized compounds. After removing the culture medium, each well received 100 L of MTT [3-(4,5-dimethylthiazol-2-yl)-3,5-diphenyltetrazolium

bromide] (Hi-Media) solution and was incubated at 37°C for 4 hours. The formazan crystals were dissolved by adding 50 L of DMSO to each well after the supernatant had been removed. This process took 10 minutes. A multiwell plate reader for the ELISA test was used to measure the optical density at 620 nm (Thermo Multiskan EX, USA). The OD value was converted to a percentage by using the algorithm below to determine viability.

% of viability = OD value of experimental sample/OD value of experimental control ×100

2.8 Statistical Analysis

An analysis of variance was performed on all data (ANOVA). The LC50 and LC90 values, as well as their 95% confidence limits, were calculated by fitting a probit regression model to the observed relationship between the logarithmic concentration of the substance and the percent mortality of the larvae. SPSS software version 16.0 was used for all analyses.

3. RESULTS AND DISCUSSION

3.1 GC-MS Analysis

The ethanolic extract of *A. cornyzoids* was subjected for GC-MS analysis showed about seven active compounds as the major peaks. The bioactive phytoconstituents with their retention time (RT), molecular formula (MF), molecular weight (MW) and peak area (%) were given in Table 1 and Fig. 1.

Table 1. Biologically active phytoconstituents of ethanolic extract of the *Ageratum cornyzoids*

No.	RT (Min)	Name of the compound	Molecular formula	Molecular weight	Peak area (%)
1	17.654	1-Oxaspiro [2.5] oct-5-ene, 8,8-dimethyl-4-methylene	C ₁₀ H ₁₄ O	150	8.078
2	17.929	1,4,4,7A-Tetramethyl-2,4,5,6,7,7A-hexahydro-1h-indene-1,7-diol	C ₁₃ H ₂₂ O ₂	210	13.383
3	18.510	2-[4-Methyl-6-(2,6,6-trimethylcyclohex-1-enyl) hexa-1,3,5-trienyl] cyclohex-1-en-1-carboxaldehyde	C ₂₃ H ₃₂ O	324	21.218
4	19.040	(1R,2R,8AS)-2,4,4,7A-Tetramethyl-1-(3-oxobutyl)-trans-hydrindan-2-carboxylic acid	C ₁₈ H ₃₀ O ₃	294	10.983
5	19.655	N-Hexadecenoic acid	C ₁₆ H ₃₂ O ₂	256	4.679
6	20.921	3-Dodecen-1-ol	C ₁₂ H ₂₄ O	184	41.659
7	31.055	2(3H)-Furanone, 3-(15-hexadecynylidene) dihydro-4-hydroxy-5-methyl-,4R-(3E,4.ALPHA.,5. BETA.)-	C ₁₂ H ₂₃ O ₂ N	213	42.90

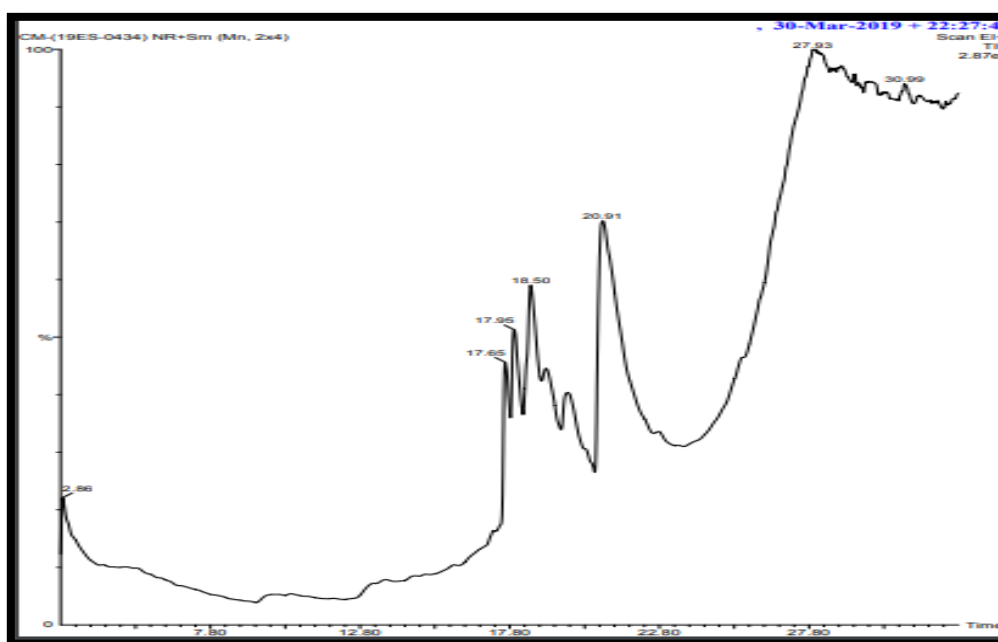


Fig. 1. GC-MS spectral analysis of the ethanol leaf extract of *Ageratum conyzoides*

The Vellore Institute of Technology (VIT) research library's recognised substances were compared to the mass spectra obtained from the GC-MS chromatogram. The substances that produced these peaks in the chromatogram were I 1-oxaspiro[2.5] Octa-5-ene, (ii) 8,8-dimethyl-4-methylene, (iii) 1,4,4-hexamethyl-2,4,5,6,7,7a-indene-1,7-diol, and (iv) 2-[4-methyl-6-(2,6,6-trimethylcyclohex-1-enyl)-hexa-1,3,5-trienyl] (iv) Cyclohex-1-ene-1-carboxaldehyde (1R,2R,8AS) - 2,4,4,7A-tetramethyl-1-(3-oxobutyl) N-hexadecanoic acid and trans-hydrindane-2-carboxylic acid (vi) Dodecen-1-ol (3-DO) and (vii) 2(3H)-furanone,3-(15-hexadecynylidene) The compound dihydro-4-hydroxy-5-methyl -4r-(3e,4,5)

The presence of alkenes, aliphatic fluorine compounds, alcohols, ethers, carboxylic acids, esters, nitro compounds, alkanes, aldehydes, and ketone compounds was demonstrated by an ethanolic extract of the leaves of *A. conyzoides*, with main peaks at 17.95, 18.50, 20.91, and 27.93. Based on gas chromatography-mass spectrometry analysis, Han [10] discovered that the main constituent of the essential oil from the invasive plant, *Ambrosia artemisiifolia*, was rich in sesquiterpenes (62.51%), with germacrene D (32.92%), -pinene (15.14%), limonene (9.90%), and caryophyllene (4.49%) being the main compounds.

3.2 UV-Visible Absorption Spectroscopy Studies

A UV-Vis spectrophotometer was used to detect the formation of silver nanoparticles in the filtrate of an aqueous extract of *A. conyzoides*. The bioreduction of Ag⁺ ions in solutions was tracked by taking aliquots (1 mL) of the aqueous component after a 20-fold dilution and measuring the UV-Vis spectra of the solutions on a regular basis. On a Shimadzu 1601 spectrophotometer with a resolution of 1 nm in the range 250-750 nm, the UV-Vis spectra of these aliquots were monitored as a function of reaction time.

The observed surface plasmon peak confirmed the effect of the *A. conyzoides* extract on the reduction of Ag⁺ to AgNP at 420 nm which steadily increased with the reaction time and became saturated after 90 min, indicating the reduction process in completely silver nitrate. "In support of our results, Kalaimurugan [11] reported that the synthesized AgNPs were initially confirmed by UV-visible spectrophotometer, and Pirtarighat [12] also observed that the surface plasmon resonance (SPR) of silver was occurs at 450 nm. The color of the mixture of *A. conyzoides* peel aqueous extract and AgNO₃ solution was determined by visual observation".

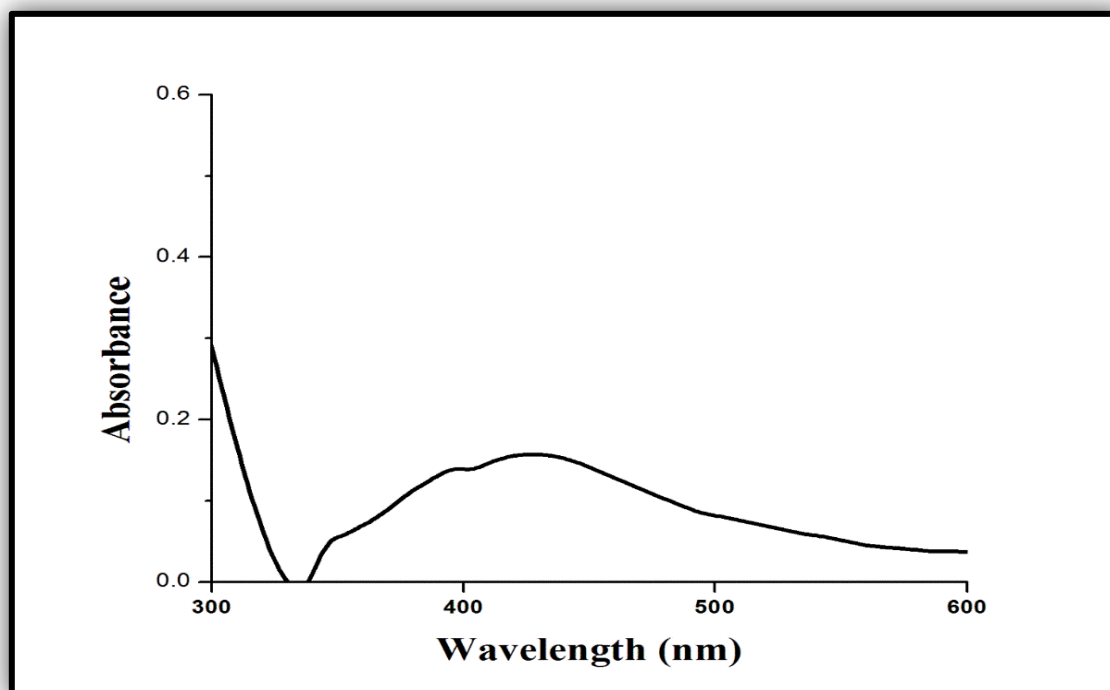


Fig. 2. UV Visible spectra recorded as the function of concentration of *A. conyzoides* leaf extract in a reaction with an aqueous solution of 1mM AgNO₃

The observed surface plasmon peak at 420 nm confirmed the effect of the *A. conyzoides* extract on Ag⁺ to AgNP reduction, which increased steadily with reaction time and became saturated after 90 minutes, indicating the reduction process in total silver nitrate. “In support of our findings, Kalaimurugan [11] reported that the synthesised AgNPs were first confirmed by a UV-Vis spectrophotometer, and Pirtarighat [12] discovered that silver has a surface plasmon resonance (SPR) at 450 nm”.

3.3 Fourier Transform Infrared Spectroscopy (FTIR) Studies

For Fourier transform infrared spectroscopy (FTIR) measurements, after complete reduction of AgNO₃ by the leaf extract of *A. conyzoides*, the reaction mixture was centrifuged at 15,000 rpm for 15 minutes to separate Ag nanoparticles from biomass or other bioorganic compounds. the protein-AgNPs can interfere with interaction. After centrifugation, the Ag nanoparticle pellet was redispersed in water and washed three

times (centrifugation and redispersion) with distilled water. Finally, the samples were dried and ground with KBr pellets before being analyzed by FTIR. These spectroscopic studies were used to search for potential bioreductants in the extract. The spectra of the extracts were recorded before and after the addition of silver nitrate solution (Fig. 3).

Both interferograms show a width at 3436 cm⁻¹, which is assigned to the NH group from the peptide bond present in the extract. The formation of C=C bonds is energetically favored over S=C bonds, since the latter impose strict geometric constraints on the molecule, more specific in the thiol group and less acidic compared to alcohols, and this leads to the elimination of hydrogen, the attached to the sulfur group. After the formation of silver nanoparticles, the concentration of amide bond in the aqueous solution decreases. In any case, the synthesised solutions of AgNPs contained many molecules, and some of them are bound or adsorbed to the surface of AgNPs.

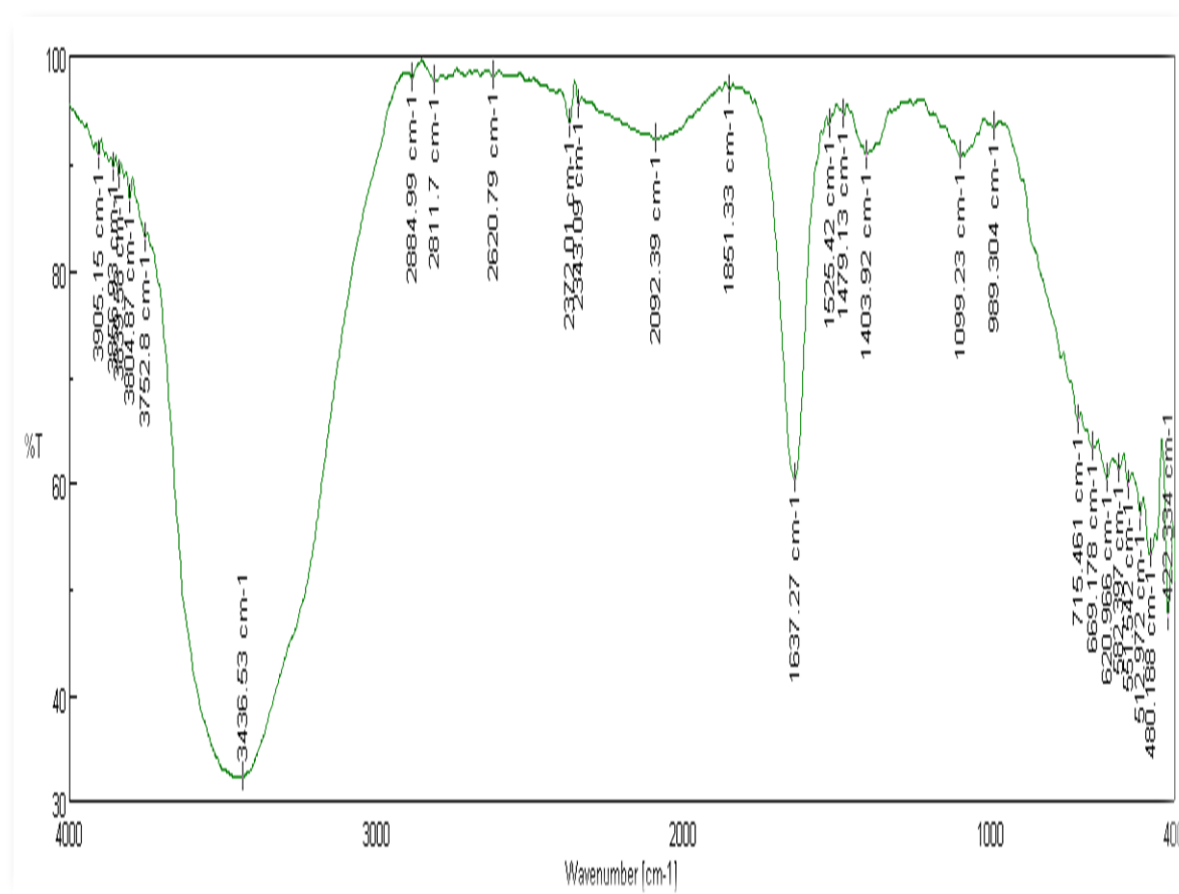


Fig. 3. FTIR Pictogram of *A. conyzoides* Synthesized silver nanoparticles

FTIR analysis confirmed that the bio-reduction of Ag^+ ions to Ag NPs is due to reduction by plant extract capping material. Because the strength of absorption is proportional to concentration, FTIR was also used for quantitative analysis in this study. These compounds may be responsible for the production of AgNPs from *A. conyzoides* leaves. Stretching frequencies were observed in the FTIR spectra of aqueous silver nanoparticles prepared from *A. conyzoides* leaf extract at 3436, 2884, 2372, 2092, 1637, 1525, and 1099 cm^{-1} . Vinoth [13] identified putative biomolecules in Sp-AgNPs using FTIR analysis, and the results revealed the presence of secondary amines, aromatic primary amines, carboxylates, amides, alkenes, aromatics, alkyne stretches, and OH stretches. The FT-IR of AgNPs obtained from the Achrassapota plant finds an expansive peak at 2800 cm^{-1} , indicating the proximity of moisture with moisture content, and the peak at 1500 cm^{-1} can be attributed on some evidence, according to Lagashetty [14]. The ridge below 1000 cm^{-1} could be caused by Ag metal particles, confirming the AgNPs arrangement.

3.4 SEM and EDX Studies

Using SEM, the samples' morphological characterizations were carried out (JEOL model 6390). An affine probe is used in the SEM to focus an electron beam, which is then raster scanned over a small rectangular region. The interaction between the beam and the sample results in a variety of signals that may all be properly detected, including secondary electrons, internal currents, photon emission, etc. According to the scanning electron microscopy, the silver nanoparticles shape was seen to be generally spherical and that they exist in aggregated form at 1.0 μm . (Fig. 4). Oves [15] stated that the thin layer supports the function of plant extract metabolites in the production and stabilisation of the biosynthesized Ag NPs, which is consistent with our findings.

The size of the produced AgNPs of *A. conyzoides* was measured at 55-80 nm, and it is depicted in representative SEM micrographs in Figs. 4 and 5, respectively. According to our findings, which have been discussed by

Lagashetty [14], the image shows random produced nanoparticles with thick and less structured particle agglomeration. EDX pattern of AgNps made from plant extracts of *Achras sapota*, *Psidium guajava*, and *Azadirachta*

indica. The entire EDX design illustrates the closeness of particle signals at particular KeV estimates. The placement of AgNp nanoparticles with diverse plant extracts is confirmed by the closeness of the indicators in the EDX.

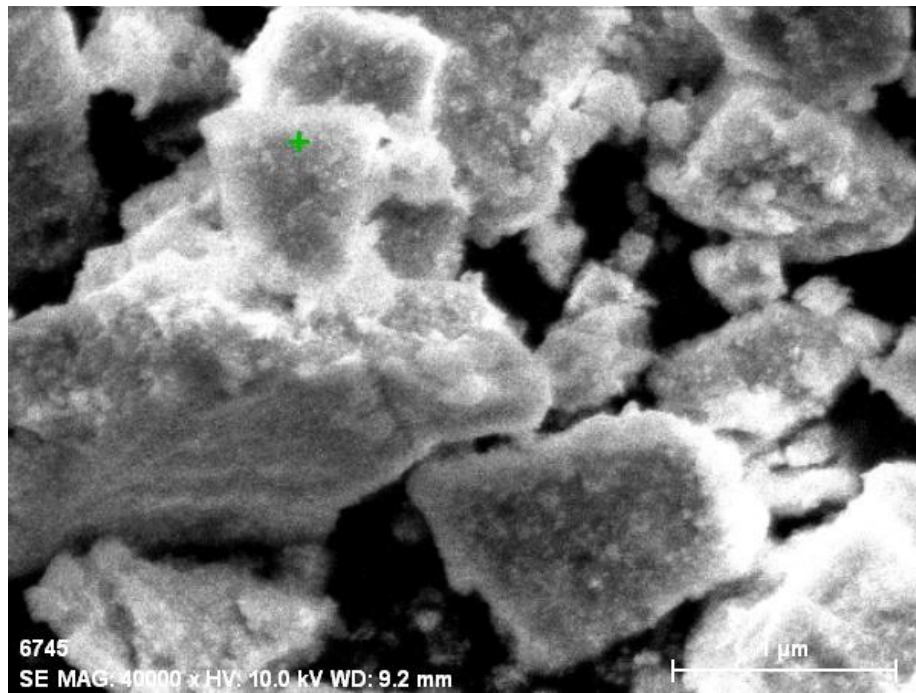


Fig. 4. SEM (Scanning electron microscope) Image of Silver nanoparticles mediated by *A. conyzoides*

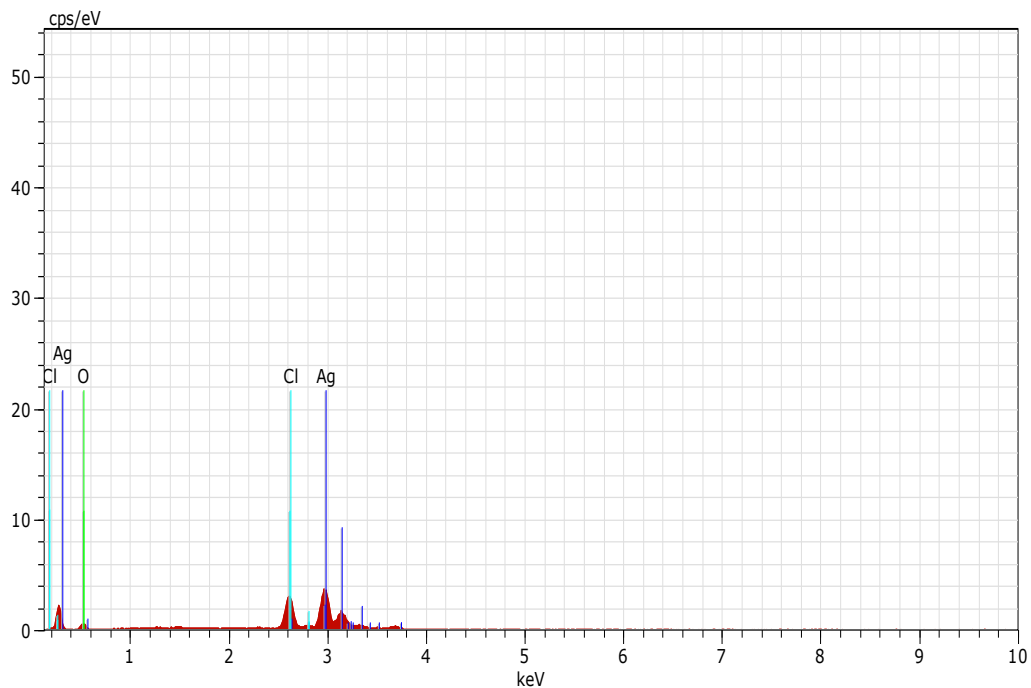


Fig. 5. Indicates the EDX pattern of *A. conyzoides* silver nanoparticles

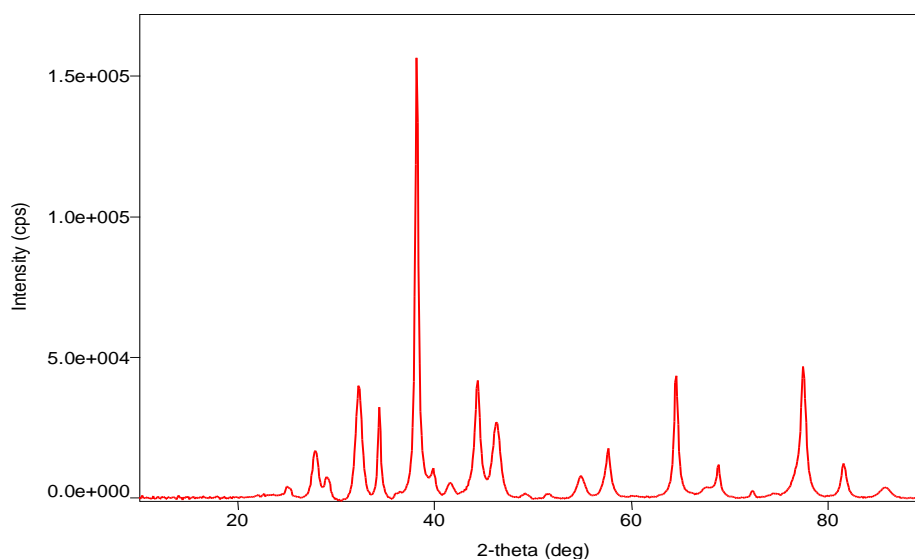


Fig. 6. Indicates the XRD pattern of *A. conyzoides* reduced silver nanoparticles

3.5 XRD Studies

The pattern of X-ray diffraction of silver nanoparticles produced by leaf extract is shown in (Fig. 6). The XRD analysis of the Ag⁺ sample exposed to *A. conyzoides* leaf broth confirmed the UV-Vis results. After the reaction, the diffraction peaks formed facets of the face-centered cubic crystal structure. Near the characteristic peaks, a few unassigned peaks were also discovered. These sharp Bragg peaks could be caused by the capping agent supporting the nanoparticle.

These peaks are associated with the face-centered cubic lattice [16]. Other peaks at 2 values in the AgNPs pattern can be attributed to plant extract organic residues. According to Shanmuganathan [17], these peaks indicate crystallisation of some plant metabolite units on the surface of AgNPs. This is sufficient evidence to suggest that plant extract compositions play a role in AgNP formation. This result is consistent with the XRD analysis [15]. Plant metabolites containing OH, CO, and especially COO, such as carnosic acid, flavonoids, and proteins, can be concluded to play an important role in the putative mechanism of silver ion bio-reduction.

3.6 Larvicidal and Pupicidal Activity of *Ae. Aegypti*

Table 2 shows the larvicidal and pupicidal activity of ethanol extracts from *A. conyzoides* leaves at various concentrations against the dengue vector

Ae. aegypti. *A. conyzoides* treatment resulted in significant mortality for all larval and pupal stages. Mortality was increased as concentration increased, for example, 27.4% mortality was noted at I instar larvae by the treatment of *A. conyzoides* at 100ppm whereas; it has been increased to 94.6% at 500ppm of *A. conyzoides* treatment. Similarly, the same trend has been noted for all larval stages and pupae of *Ae. aegypti* at different concentrations (100, 200, 300, 400 and 500 ppm) The LC₅₀ and LC₉₀ values represented as follows: LC₅₀ was found to be I (92.9) ppm, II (267.5) ppm, III (307.680) ppm, IV (363.302) ppm and for pupa (421.560) ppm, respectively. LC₉₀ value of I instar was 487.116 ppm, II instar was 551.65 ppm, III instar was 307.68 ppm, IV instar was 708.93 ppm, and pupa was 807.92 ppm, respectively. Table 3 Effect of *A. conyzoides* plant extract with AgNPs on the larvae and pupae of *Ae. aegypti* are shown in various concentrations (10, 20, 30, 40 and 50ppm) of *A. conyzoides* with AgNps treated against the dengue mosquito *Ae. aegypti* exhibited toxic effects and produced mortality ranging between 31.2 and 97.3% in first instar, 27.3–93.4% in second Instar, 24.6– 84.8% in third instar, 18.78- 72.1% in fourth instar, 14.0– 61.3% in the pupae at different concentrations ranging from 10 to 50ppm. The LC₅₀ and LC₉₀ values represented as follows: LC₅₀ value of I was (20.451) ppm, II was (23.307) ppm, III was (27.397) ppm, IV was (33.351) ppm and pupa was 39.668 ppm, respectively. LC₉₀ value of I was (44.240) ppm, II was (549.268) ppm, III was (57.450) ppm, IV was (68.671) ppm, and pupa was 78.353 ppm, respectively.

Similarly, Gaal [18] reported that *Ae. albopictus* larvae and pupae were tested against green synthesis of silver nanoparticles using *Ustilago maydis*. With LC₅₀ values ranging from 1.03 to 1.19 g/mL, AgNPs were most toxic to *Ae. albopictus* larvae and pupae. Nalini [19] discovered that phytosynthesized AgNPs had

potent larvicidal and pupicidal activity against the developmental stages of *An. stephensi* and *Ae. aegypti* (larval and pupal stages I-IV). Insecticidal biomolecules derived from natural resources (*Champia parvula*) have been shown to have potent mosquito-killing (*Ae. aegypti*) and insecticidal properties, according to Yogarajalakshmi [20].

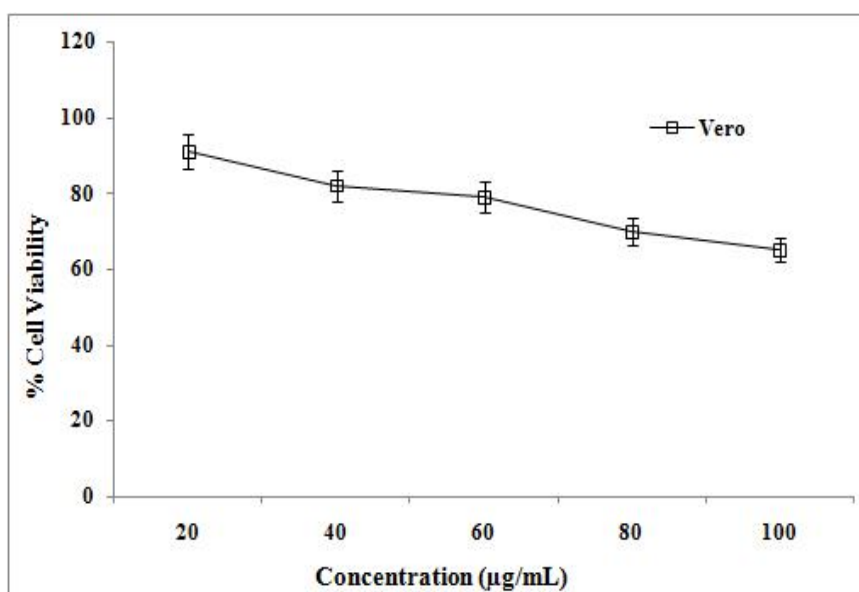


Fig. 7. Cytotoxic effect of *A. conyzoides*-synthesized Ag nanoparticles on Vero cell

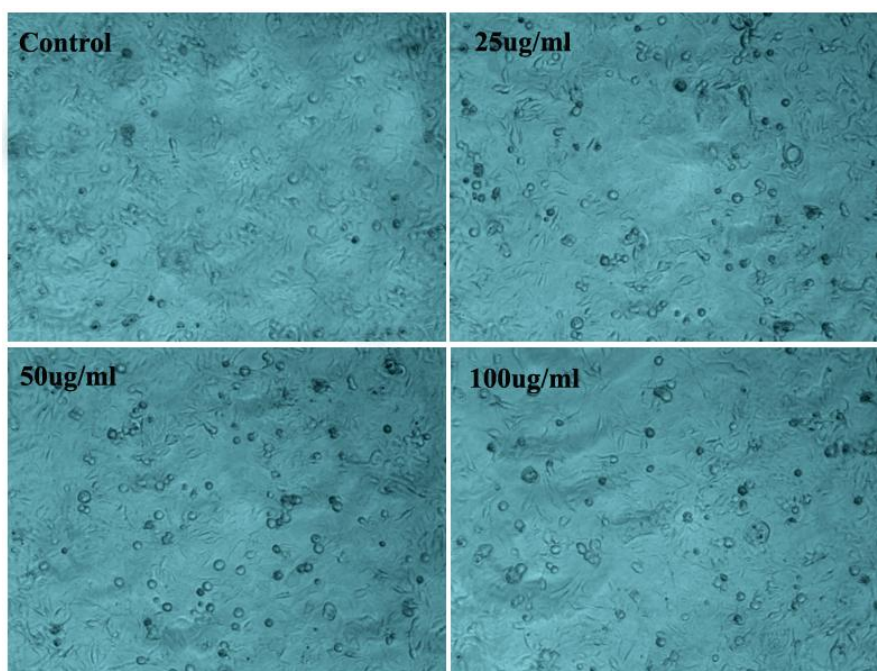


Fig. 8. Vero cell viability after the treatment with *A. conyzoides*-synthesized AgNPs (25, 50 and 100 µg/ml) after 24h

Table 2. Larval and pupal toxicity effect of ethanolic leaves extract of *A. conyzoides* against dengue vector *Aedes aegypti*

Target	Percentage of larval and pupal mortality (%)					LC ₅₀ and (LC ₉₀)	95% confidence limit		Regression equation	χ ² (d.f.=4)
	Concentration (ppm)						LC ₅₀ (LC ₉₀)			
	100	200	300	400	500		LCL	UCL		
I Instar	27.4± 2.2 ^a	43.2± 0.64 ^b	61.2± 1.02 ^c	76.2± 1.14 ^d	94.6± 0.75 ^e	92.895 (487.116)	206.741 (447.350)	258.298 (541.864)	y = -1.185+0.005x	2.925 ^{n.s}
II Instar	24.4±0.92 ^a	38.4± 0.82 ^b	54.2±0.76 ^c	70.2±.76 ^d	87.8±0.84 ^e	267.467 (551.658)	239.396 (502.352)	293.710 (622.024)	y= -1.206+0.005 x	1.082 ^{n.s}
III Instar	19.8± 1.13 ^a	32.4± 0.22 ^b	50.4 ±0.68 ^c	63.8±.46 ^d	79.30±0.48 ^e	307.680 (617.992)	279.030 (557.507)	336.872 (707.399)	y= -1.271+0.004 x	0.155 ^{n.s}
IV Instar	15.4± 0.76 ^a	27.8± 1.02 ^b	43.4±0.54 ^c	55.6±0.49 ^d	68.4±0.88 ^e	363.302 (708.937)	331.626 (629.338)	400.690 (833.213)	y= -1.347+0.004 x	0.475 ^{n.s}
Pupa	12.2±0.54 ^a	24.8±0.47 ^b	36.2± 0.28 ^c	49.2±0.60 ^d	57.6± 0.70 ^e	421.560 (807.926)	382.607 (702.388)	475.277 (984.135)	y= -1.398+0.003 x	1.149 ^{n.s}

Mortality rates are means ± SD of three replicates; LC50 = lethal concentration that kills 50% of the exposed organisms; LC90 = lethal concentration that kills 90% of the exposed organisms; LCL = Lower Confidence Limit; UCL = Upper Confidence Limit; χ² = chi-square; n.s. = not significant (α = 0.05) Values followed by the same letter(s) are not significantly different (DMRT, α = 0.02)

Table 3. Larval and pupal toxicity effect of synthesise AgNPs using *A. conyzoides* against dengue vector *Aedes aegypti*

Target	Percentage of larval and pupal mortality (%)					LC ₅₀ and (LC ₉₀)	95% confidence Limit		Regression equation	χ ² (d.f.=4)
	Concentration (ppm)						LC ₅₀ (LC ₉₀)			
	10	20	30	40	50		LCL	UCL		
I Instar	31.2±0.25 ^a	49.4± 0.53 ^b	66.0± 0.60 ^c	83.6± 0.71 ^d	97.3±086 ^e	20.451 (44.240)	17.632 (40.713)	22.861 (49.024)	y = -1.102+0.054x	2.408 ^{n.s}
II Instar	27.3±0.66 ^a	44.7± 0.45 ^b	59.2±1.03 ^c	77.8±0.61 ^d	93.4±0.89 ^e	23.307 (49.268)	20.499 (45.170)	25.790 (54.946)	y= -1.151+0.049 x	1.638 ^{n.s}
III Instar	24.6± 0.48 ^a	36.1± 0.77 ^b	54.2 ±0.62 ^c	69.4±0.43 ^d	84.8±0.55 ^e	27.397 (57.450)	24.475 (52.044)	30.154 (65.313)	y= -1.168+0.043 x	0.556 ^{n.s}
IV Instar	18.5± 0.76 ^a	32.2± 0.95 ^b	47.6± 0.44 ^c	58.7±0.47 ^d	72.1±0.87 ^e	33.351 (68.671)	30.169 (60.928)	36.843 (80.786)	y= -1.210+0.036 x	0.424 ^{n.s}
Pupa	14.0± 0.15 ^a	27.5± 0.35 ^b	39.4± 0.51 ^c	52.2±0.99 ^d	61.3± 0.28 ^e	39.668 (78.353)	35.984 (68.292)	44.497 (95.020)	y= -1.314+0.033 x	0.994 ^{n.s}

Mortality rates are means ± SD of three replicates; LC50 = lethal concentration that kills 50% of the exposed organisms; LC90 = lethal concentration that kills 90% of the exposed organisms; LCL = Lower Confidence Limit; UCL = Upper Confidence Limit; χ² = chi-square; n.s. = not significant (α = 0.05) Values followed by the same letter(s) are not significantly different (DMRT, α = 0.02)

3.7 Antiviral Activity

In this study, the anti-dengue properties of *A. conyzoides* synthesized AgNPs, *in vitro* antiviral assay was conducted. The current study found moderate cytotoxicity rates in Vero cells exposed to plant-derived AgNPs at concentrations less than 4 µg ml⁻¹. Indeed, after the treatment, less than 30 % of the treated cells showed no viability (Fig. 7). Furthermore, plant-tested at 25-100 µg/ml significantly inhibit DEN-2 replication, resulting in a decrease in PFU abundance (Fig. 8). In the current study, the viability of vero cells exposed to different doses of extract. From that we observed there is no any adverse morphological differences were found in the treated cells comparable to the control vero cells. Previous study reports that a range of extract, exhibited significant cytotoxicity against HEK cell with less than 30% viability at a concentration of 100 µg/ml. Cytotoxic effects of extract on MDCK cells were reported that more than 60µM concentration cause severe cell death in *in vitro* condition [21].

Recent research has highlighted the potential of metal nanoparticles as growth inhibitors for the DEN-2 gene [22], which supports our findings. Ag nanoparticles suppress the DEN-2 E gene's expression [23]. On the other hand, moderate toxicity of the tested Ag nanoparticles has been reported (for example, fifty µg ml⁻¹ semiconductor diode to a discount of half an hour in cell viability). Then, *Centrocera sclavulatum*-fabricated Ag nanoparticles tested at 50 µgml⁻¹ failed to show significant cytotoxicity, while these inhibited the growth of DEN-2 by 80% [24]. Again, the results previously mentioned highlighted the crucial potential of thoroughly screening a variety of botanic and microbial resources for parasitological functions [25,26].

4. CONCLUSION

As a result of our findings, we hypothesise that the synthesised silver nanoparticles mediated by *A. conyzoides* may also mediate anti-dengue activity. Henceforth, *A. conyzoides* synthesized silver nanoparticles would be regarded as a better means of treating the infectious disease caused by dengue virus and dengue vector *Ae. aegypti* tested in the field of modern research dealing with particle design, synthesis, and manipulation. As a result, work on nanoparticles is of interest, and more attention is being paid to producing nanoparticles using plant biomass in environmentally friendly ways (green chemistry).

COMPETING INTERESTS

Authors have declared that no competing interests exist.

REFERENCES

1. Bhatt S, Gething PW, Brady OJ, Messina JP, Farlow AW, Moyes et al. The global distribution and burden of dengue. *Nature*. 2013;496(7446):504-507.
DOI:<https://doi.org/10.1038/nature12060>
2. WHO. Dengue and severe dengue. Fact sheet N117; 2015. Updated May 2015
3. Sujitha V, Murugan K, Dinesh D, Pandiyan A, Aruliah R, Hwang JS, et al. Green-synthesized CdS nano-pesticides: toxicity on young instars of malaria vectors and impact on enzymatic activities of the non-target mud crab *Scylla serrata*. *Aquatic Toxicology*. 2017;188:100-108.
DOI:<https://doi.org/10.1016/j.aquatox.2017.04.015>
4. Amerasan D, Nataraj T, Murugan K, Panneerselvam C, Madhiyazhagan P, Nicoletti M et al. Myco-synthesis of silver nanoparticles using *Metarhizium anisopliae* against the rural malaria vector *Anopheles culicifacies* Giles (Diptera: Culicidae). *Journal of Pest Science*. 2016;89(1):249-256.
DOI:<https://doi.org/10.1007/s10340-015-0675-x>
5. Kumar S, Lather V, Pandita D. Green synthesis of therapeutic nanoparticles: an expanding horizon. *Nanomedicine*. 2015;10(15):2451-2471.
DOI:<https://doi.org/10.2217/nnm.15.112>
6. Kamboj A, Saluja AK. *Ageratum conyzoides* L.: A review on its phytochemical and pharmacological profile. *International Journal of Green Pharmacy (IJGP)*. 2008.2(2).
DOI:<https://doi.org/10.22377/ijgp.v2i2.29>
7. Sridharan S, Meenaa V, Kavitha V, Nayagam AAJ. GC-MS study and phytochemical profiling of *Mimosa pudica* Linn. *Journal of Pharmacy Research*. 2011;4(3):741-2.
8. Dinesh D, Murugan K, Madhiyazhagan P, Panneerselvam C, Mahesh Kumar P, Nicoletti M, et al. Mosquitocidal and antibacterial activity of green-synthesized silver nanoparticles from *Aloe vera* extracts: towards an effective tool against the malaria vector *Anopheles stephensi*?

- Parasitology Research. 2015;114:1519-1529.
9. Kovendan K, Chandramohan B, Dinesh D, Abirami D, Vijayan P, Govindarajan M, et al. Green-synthesized silver nanoparticles using *Psychotria nilgiriensis*: toxicity against the dengue vector *Aedes aegypti* (Diptera: Culicidae) and impact on the predatory efficiency of the non-target organism *Poecilia sphenops* (Cyprinodontiformes: Poeciliidae). *Journal of Asia-Pacific Entomology*. 2016;19(4):1001-1007. DOI:<https://doi.org/10.1016/j.aspen.2016.09.001>
 10. Han C, Shao H, Zhou S, Mei Y, Cheng Z, et al. Chemical composition and phytotoxicity of essential oil from invasive plant *Ambrosia artemisiifolia* L. *Ecotoxicology and Environmental Safety*. 2021;211:111879. DOI:<https://doi.org/10.1016/j.ecoenv.2020.111879>
 11. Kalaimurugan D, Vivekanandhan P, Sivasankar P, Durairaj K, Senthilkumar P, Shivakumar MS, et al. Larvicidal activity of silver nanoparticles synthesized by *Pseudomonas fluorescens* YPS3 isolated from the Eastern Ghats of India. *Journal of Cluster Science*. 2019;30(1):225-233. DOI:<https://doi.org/10.1007/s10876-018-1478-z>
 12. Pirtarighat S, Ghannadnia M, Baghshahi S. Green synthesis of silver nanoparticles using the plant extract of *Salvia spinosa* grown in vitro and their antibacterial activity assessment. *Journal of Nanostructure in Chemistry*. 2019;9(1):1-9. DOI:<https://doi.org/10.1007/s40097-018-0291-4>
 13. Vinoth S, Shankar S.G, Gurusaravanan P, Janani B, Devi JK. Anti-larvicidal activity of silver nanoparticles synthesized from *Sargassum polycystum* against mosquito vectors. *Journal of Cluster Science*. 2019;30(1):171-180. DOI:<https://doi.org/10.1007/s10876-018-1473-4>
 14. Lagashetty A, Patil MK, Ganiger SK. Green synthesis characterization and thermal study of silver nanoparticles by *Achras sapota* *Psidium guajava* and *Azadirachta indica* plant extracts. *Plasmonics*. 2019;14(5):1219-1226. DOI:<https://doi.org/10.1007/s11468-019-00910-3>
 15. Oves M, Aslam M, Rauf M.A, Qayyum S, Qari HA, et al. Antimicrobial and anticancer activities of silver nanoparticles synthesized from the root hair extract of *Phoenix dactylifera*. *Materials Science and Engineering: C*. 2018;89:429-443. DOI:<https://doi.org/10.1016/j.msec.2018.03.035>
 16. Estévez M, Luna C. Dietary protein oxidation: A silent threat to human health?. *Critical Reviews in Food Science and Nutrition*. 2017;57(17):3781-3793. DOI:<https://doi.org/10.1080/10408398.2016.1165182>
 17. Shanmuganathan R, MubarakAli D, Prabakar D, Muthukumar H, Thajuddin N, Kumar SS, et al. An enhancement of antimicrobial efficacy of biogenic and ceftriaxone-conjugated silver nanoparticles: green approach. *Environmental Science and Pollution Research*. 2018;(11):10362-10370. DOI:<https://doi.org/10.1007/s11356-017-9367-9>
 18. Ga'al H, Yang G, Fouad H, Guo M, Mo J. Mannosylerythritol lipids mediated biosynthesis of silver nanoparticles: an eco-friendly and operative approach against chikungunya vector *Aedes albopictus*. *Journal of Cluster Science*. 2021;32(1):17-25. DOI:<https://doi.org/10.1007/s10876-019-01751-0>
 19. Nalini M, Lena M, Sumathi P, Sundaravadivelan C. Effect of phyto-synthesized silver nanoparticles on developmental stages of malaria vector *Anopheles stephensi* and dengue vector *Aedes aegypti*. *Egyptian Journal of Basic and Applied Sciences*. 2017;4(3):212-218. DOI:<https://doi.org/10.1016/j.ejbas.2017.04.005>
 20. Yogarajalakshmi P, Poonguzhali TV, Ganesan R, Karthi S, Senthil-Nathan S, Krutmuang P, et al.. Toxicological screening of marine red algae *Champia parvula* (C. Agardh) against the dengue mosquito vector *Aedes aegypti* (Linn.) and its non-toxicity against three beneficial aquatic predators. *Aquatic Toxicology*. 2020;222:105474. DOI:<https://doi.org/10.1016/j.aquatox.2020.105474>
 21. Paulpandi M, Kavithaa K, Sumathi S, Padma PR. Increased anticancer efficacy by the combined administration of

- quercetin in multidrug resistant breast cancer cells. *Annals of Oncology*. 2013; 24:iii19.
DOI:<https://doi.org/10.1093/annonc/mdt081.4>
22. Sujitha V, Murugan K, Paulpandi M, Panneerselvam C, Suresh U, Roni M, et al. Green-synthesized silver nanoparticles as a novel control tool against dengue virus (DEN-2) and its primary vector *Aedes aegypti*. *Parasitology Research*. 2015;114(9):3315-3325.
DOI:<https://doi.org/10.1007/s00436-015-4556-2>
23. Murugan K, Benelli G, Panneerselvam C, Subramaniam J, Jeyalalitha T, Dinesh D, et al. Cymbopogon citratus-synthesized gold nanoparticles boost the predation efficiency of copepod *Mesocyclops aspericornis* against malaria and dengue mosquitoes. *Experimental Parasitology*. 2015;153:129-138.
DOI:<https://doi.org/10.1016/j.exppara.2015.03.017>
24. Murugan K, Aruna P, Panneerselvam C, Madhiyazhagan P, Paulpandi M, Subramaniam J, et al. Fighting arboviral diseases: low toxicity on mammalian cells dengue growth inhibition (in vitro) and mosquitocidal activity of *Centrocercus clavulatum*-synthesized silver nanoparticles. *Parasitology Research*. 2016;115(2):651-662.
DOI:<https://doi.org/10.1007/s00436-015-4783-6>
25. Benelli G. Plant-borne ovicides in the fight against mosquito vectors of medical and veterinary importance: a systematic review. *Parasitology Research*. 2015;114(9):3201-3212.
DOI:<https://doi.org/10.1007/s00436-015-4656-z>
26. Benelli G Plant-mediated biosynthesis of nanoparticles as an emerging tool against mosquitoes of medical and veterinary importance: a review. *Parasitology Research*. 2016;115(1):23-34.
DOI:<https://doi.org/10.1007/s00436-015-4800-9>